Evaluation of the influences of solution path length and additives concentrations on the solar photo-Fenton degradation of 4-chlorophenol using multivariate analysis

Alam G. Trovó, Willian C. Paterlini, Raquel F. Pupo Nogueira *

UNESP, São Paulo State University, Institute of Chemistry of Araraquara, Department of Analytical Chemistry, CP 355, 14801-970 Araraquara, SP, Brazil

Abstract

This study reports the photodegradation of 4-chlorophenol (4-CP) in aqueous solution by the photo-Fenton process using solar irradiation. The influence of solution path length, and $Fe(NO_3)_3$ and H_2O_2 concentrations on the degradation of 4-CP is evaluated by response surface methodology. The degradation process was monitored by the removal of total organic carbon (TOC) and the release of chloride ion. The results showed a very important role of iron concentration either for TOC removal or dechlorination. On the other hand, a negative effect of increasing solution path length on mineralization was observed, which can be compensated by increasing the iron concentration. This permits an adjustment of the iron concentration according to the irradiation exposure area and path length (depth of a tank reactor). Under optimum conditions of 1.5 mM $Fe(NO_3)_3$, 20.0 mM H_2O_2 and 4.5 cm solution path length, 17 min irradiation under solar light were sufficient to reduce a 72 mg C L^{-1} solution of 4-CP by 91%.
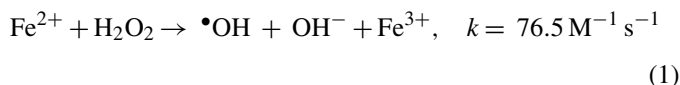© 2006 Elsevier B.V. All rights reserved.

Keywords: Advanced oxidation processes; Degradation; 4-Chlorophenol; Experimental design

1. Introduction

Chlorinated compounds are highly toxic and persistent substances which tend to accumulate in the environment, causing diverse collateral effects in the nervous systems of a variety of organisms [1,2]. Among chlorinated compounds, chlorophenols are considered priority pollutants by EPA and represent a special threat to aqueous environments and public health due to their relatively high solubility in water. Consequently, it is necessary to take steps for the development and application of economic, simple and efficient processes for the destruction of these compounds in parallel to the minimization of their use [3].

Generally organic compounds are removed from water using granular carbon or activated carbon, nanofiltration, ozonation, and by biodegradation with specific bacterial cultures. However, while some of these processes are only efficient in transferring the problem to another phase, others present limitations in the applicability, effectiveness or cost [4–7].

Advanced oxidation processes (AOP) have attracted great interest due to their high efficiency in the oxidation of a variety of compounds due to the generation of hydroxyl radicals ($^{\bullet}$OH). The Fenton reaction (Eq. (1)) has been used as a powerful source of hydroxyl radicals released by the decomposition of H_2O_2 in the presence of ferrous ions. The combination of the Fenton reaction with light (Eq. (2)) increases the efficiency of the process due to the decomposition of the photo-active $Fe(OH)^{2+}$, leading to important additional $^{\bullet}$OH radicals in solution and cyclic regeneration of Fe^{2+}. Both Fenton and photo-Fenton are considered suitable processes for the treatment of wastewaters containing high concentrations of chlorophenols in water due to the high efficiency of oxidation at low cost [8,9].

$$Fe^{2+} + H_2O_2 \rightarrow {}^{\bullet}OH + OH^- + Fe^{3+}, \quad k = 76.5\,M^{-1}\,s^{-1}$$

(1)

$$Fe(OH)^{2+} + h\nu \rightarrow Fe^{2+} + {}^{\bullet}OH$$

(2)

Moreover, it is possible to use solar energy as source of irradiation in the photo-Fenton process, reducing energy costs [10–12].

---

* Corresponding author. Tel.: +55 16 3301 6606; fax: +55 16 3322 7932.
  E-mail address: nogueira@iq.unesp.br (R.F.P. Nogueira).

Multivariate analysis has been recently applied for the evaluation of the parameters involved in the degradation reactions, such as iron and hydrogen peroxide concentrations in the photo-Fenton process. A quadratic model is generally applied, in which the synergistic and antagonist effects between the variables are taken into account [13–16]. The initial concentrations of $Fe(NO_3)_3$ and H_2O_2 are important variables to be evaluated in photo-Fenton process. The increase of iron concentration increases the absorption of the solution, which also influences the penetration of light and consequently the exposure area. The concentration of H_2O_2 in the system is a very important parameter, since at high concentrations the efficiency of the process can be reduced due to scavenging of $^\bullet OH$. The importance of evaluating the path length is to minimize the exposure area, increasing the depth of a tank reactor, for example when solar irradiation is used in this homogeneous system.

In the present work, the degradation of 4-chlorophenol (4-CP) by the photo-Fenton process using solar energy was studied. The multivariate analysis, more precisely the response surface methodology, was used to evaluate the role of the three variables, initial concentrations of $Fe(NO_3)_3$ and hydrogen peroxide and the optical path length of the irradiated solution, which is varied by the height of the photoreactor. The role of each variable was evaluated and the optimum conditions are expressed by the highest percentage of total organic carbon (TOC) removal and dechlorination of 4-CP.

2. Materials and methods

2.1. Chemicals

All the solutions were prepared with Millipore Milli-Q water and analytical grade reagents. $Fe(NO_3)_3 \cdot 9H_2O$ (Mallinkrodt) was used to prepare aqueous 0.25 M iron stock solution. H_2O_2 30% (w/w) (Merck) was used. Ammonium metavanadate (Vetec) solution was prepared at the concentration of 0.060 M in 0.36 M H_2SO_4. A 5.0 M sodium nitrate (Mallinkrodt) solution was used for ionic strength adjustment, and a 1.00 M NaCl (Mallinkrodt) solution was used as the chloride standard for the potentiometric determination of this ion. 4-CP was purchased from Merck.

2.2. Experimental design

The central composite design was used to investigate the effects of $Fe(NO_3)_3$ and H_2O_2 concentrations and the path length of solution, as well as to evaluate the interactions among these three variables. The central composite design is the result of superimposing a factorial design at two levels (2^k) (all possible combinations of codified values +1.0 and −1.0), which in the case of $k = 3$ variables consists of eight experiments, a star design ($2k + 1$), which consists of seven experiments (±1.6, 0, 0), (0, ±1.6, 0), (0, 0, ±1.6), (0, 0, 0) and three replicates on the central point (0, 0, 0). This results in investigating the following experimental ranges: iron (0.20–1.50 mM), H_2O_2 (6.0–20.0 mM) and solution path length (4.5–14.0 cm). The ranges of iron, H_2O_2 and solution path length were chosen based on the results of previous

work [11]. The equations used to quantitatively describe each system and draw the contour plots were built using STATISTICA software (SW7127999218G51), based on the experimental data obtained for TOC removal and chloride release after an accumulated UV energy dose of 2.02 J cm^{-2}.

2.3. Solar photodegradation procedure and energy dose measurements

Solar photodegradation of 4-CP solution was carried out using open dark glass vessels (without magnetic stirring) to avoid lateral penetration of light, thus enabling the evaluation of path length influence on the photodegradation processes, which was obtained by different reactor depths. The internal diameter of the vessels was 9 cm with depths varying from 4.5 to 14 cm, resulting in solution volumes from 270 to 850 mL. The experiments were undertaken in Araraquara, Brazil (21°47′S, 48°10′W) during winter and spring under clear sky conditions. The global radiation during exposure was measured using a radiometer (PMA 2100 Solar Light Co.) in the UVA region (320–400 nm) with the sensor placed horizontally. The samples for analysis were withdrawn after exposure to the same solar UV dose of 2.02 J cm^{-2} (between 13 and 15 min irradiation). The exposure of the solution to the same UV dose allows a good comparison of the results as observed in previous work [15]. The pH of each target compound solution was adjusted to 2.5 by the addition of 3 M H_2SO_4 before starting the experiments [17]. The initial concentration of 4-CP was 1.0 mM (TOC = 72 mg L^{-1}) in all experiments.

2.4. Chemical analysis

The efficiency of the photodegradation process was evaluated by the TOC removal percentages (mineralization of 4-CP) using a TOC analyzer (TOC-5000A SHIMADZU). The TOC concentration includes the carbon content of the target compound and the intermediates generated during the experiment. The photodegradation was also evaluated by the generation of chloride ions determined by direct potentiometry using the standard addition method as previously described by Nogueira et al. [11]. Chloride ion concentrations were expressed as a percentage of the total theoretical amount of these ions that can be released from the model compound. The analyses of TOC and Cl$^-$ were performed immediately after withdrawal of samples to avoid further reaction. In addition, the residual H_2O_2 concentration was determined spectrophotometrically after reaction with ammonium metavanadate [18].

3. Results and discussion

In order to effectively apply advanced oxidation processes for the abatement of contaminants, it is very important to optimize the conditions involved in the photodegradation process. The experimental conditions for all experiments and the corresponding results obtained are shown in Table 1. The results were first analyzed to determine second-order equations including the terms of interactions among three variables. Eqs. (3) and (4)

Table 1
Central composite design of photo-Fenton degradation of 4-CP (2.02 J cm^{-2}) and corresponding results obtained

Experiment	Fe^{3+} (mM)	H$_2$O$_2$ (mM)	Solution path length (cm)	Mineralization (%)	TOC removal (mg C min^{-1})	Dechlorination (%)
1	0.44 (−1)	8.6 (−1)	6.3 (−1)	38.4	0.70	92.1
2	1.26 (+1)	8.6 (−1)	6.3 (−1)	52.1	0.96	82.7
3	0.44 (−1)	17.4 (+1)	6.3 (−1)	46.5	0.86	98.0
4	1.26 (+1)	17.4 (+1)	6.3 (−1)	70.0	1.38	100
5	0.44 (−1)	8.6 (−1)	12.2 (+1)	35.7	1.24	86.4
6	1.26 (+1)	8.6 (−1)	12.2 (+1)	56.2	2.33	79.5
7	0.44 (−1)	17.4 (+1)	12.2 (+1)	37.0	1.29	89.5
8	1.26 (+1)	17.4 (+1)	12.2 (+1)	62.9	2.62	96.7
9	0.20 (−1.6)	13.0 (0)	9.2 (0)	33.6	1.02	86.0
10	1.50 (+1.6)	13.0 (0)	9.2 (0)	71.2	2.19	100
11	0.85 (0)	6.0 (−1.6)	9.2 (0)	29.3	0.90	71.1
12	0.85 (0)	20.0 (+1.6)	9.2 (0)	64.9	2.00	100
13	0.85 (0)	13.0 (0)	4.5 (−1.6)	77.2	1.11	99.1
14	0.85 (0)	13.0 (0)	14.0 (+1.6)	49.3	2.24	98.0
15	0.85 (0)	13.0 (0)	9.2 (0)	61.4	1.57	92.6
16	0.85 (0)	13.0 (0)	9.2 (0)	58.7	1.56	97.5
17	0.85 (0)	13.0 (0)	9.2 (0)	58.8	1.57	97.8
18	0.85 (0)	13.0 (0)	9.2 (0)	56.7	1.52	100
Standard deviation[a]				1.9	0.02	3.1

[a] Standard deviation of central points (experiments 15–18).

were obtained based on the statistical analysis of the percentage of TOC removal (TOC, %) and chloride release (Cl$^-$, %) from 4-CP, respectively, after exposure to an UV dose of 2.02 J cm^{-2}. The coefficients of the quadratic model in the equation were calculated by least-square multi-linear regression analysis. The importance of each variable depends on its sign and value and on the associated relative error (absolute value), which is indicated in parentheses in the equations. The coefficients which absolute values were lower than their errors were excluded from the equations. The percentage of explained variance for 95% confidence level in each system is also shown. The variables x_1, x_2 and x_3 are iron concentration, H$_2$O$_2$ concentration and solution path length, respectively.

$$(TOC, \%) = 58.97 \,(\pm 3.05) + 10.71 \,(\pm 1.68)x_1$$
$$+ 6.87 \,(\pm 1.68)x_2 - 4.55 \,(\pm 1.68)x_3$$
$$- 3.07 \,(\pm 1.80)x_1^2 - 4.94 \,(\pm 1.80)x_2^2$$
$$- 2.25 \,(\pm 2, 17)x_2x_3 \quad (89.9\%) \tag{3}$$

$$(Cl^-, \%) = 97.03 \,(\pm 4.94) + 6.74 \,(\pm 2.72)x_2$$
$$- 4.34 \,(\pm 2.92)x_2^2 \quad (88.0\%) \tag{4}$$

Analyzing Eq. (3), the high positive coefficient values of x_1 and x_2 indicate that TOC removal is favored in the presence of high concentrations of iron and H$_2$O$_2$, while the negative coefficient value of x_3 indicates that the degradation process is favored with low solution path length. The overall effect can be observed in Fig. 1, which shows the contour plots built up with the results seen in Table 1. Fig. 1A–C show the percentages of TOC removed as a function of iron and peroxide concentrations as well as solution path length. It can be observed in Fig. 1A

and B that the iron concentration plays a very important role in the degradation process, since the increase of its concentration increases the TOC removal. The increase of iron concentration also compensates for the negative effect of increasing solution path length as can be seen in Fig. 1B, since high TOC removal is obtained also with high solution path length when high iron concentrations are used. This is an interesting result especially when large areas are not available for irradiation. In this case, smaller exposure areas can be used for the treatment of a large wastewater volume by increasing the path length (depth of a tank reactor). In this case, higher iron concentration should be used to obtain an efficient treatment. On the other hand, although increasing H$_2$O$_2$ concentration increases the degradation efficiency, H$_2$O$_2$ plays a less important role than iron for the degradation of 4-CP, indicated by the lower coefficient of x_2 (+6.87) in relation to x_1 (+10.71). As can be seen in Fig. 1C, the increase of solution path length decreases the TOC removal, even when a high H$_2$O$_2$ concentration is used.

Considering that with a higher path length a higher volume of solution is treated, the absolute TOC removal (mass of carbon removed) is higher for the same percentage of TOC removed. So the mass of carbon removed per minute was calculated in each case, which ranged from 0.70 to 2.62 mg C min^{-1} (Table 1). The highest removal (2.62 mg C min^{-1}) was achieved in a 12.2 cm deep reactor, of 750 mL volume. In this case, the concentration of iron and H$_2$O$_2$ used were 1.26 mM and 17.4 mM, close to the maximum concentrations studied. However, the discharge of a residual carbon concentration of 26.7 mg C L^{-1} (37% of the initial content) would be not acceptable unless a further biological treatment is carried out, what can be advantageous.

When analyzing the dechlorination results, it can be observed that the solution path length and iron concentration play no significant role in the dechlorination compared to mineralization, as can be seen in Fig. 1E and F. High dechlorination percentages are
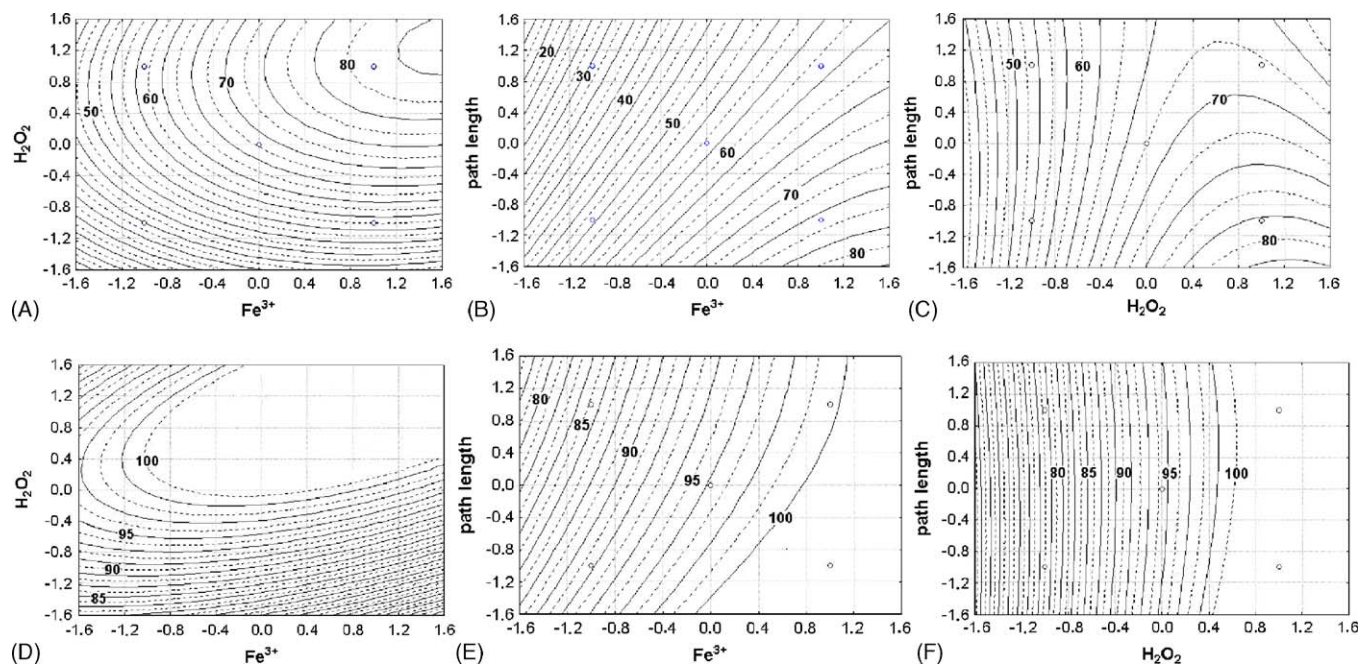
Fig. 1. Contour plots of quadratic model for mineralization and dechlorination percentages of 4-CP (1.0 mM; TOC = 72 mg L^{-1}) as a function of Fe^{3+} and H$_2$O$_2$ concentrations (A and D), Fe^{3+} concentration and solution path length (B and E), and H$_2$O$_2$ concentrations and solution path length (C and F), respectively. Fixed values: path length = 4.5 cm (A and D); [H$_2$O$_2$] = 20.0 mM (B and E); and [Fe^{3+}] = 1.5 mM (C and F).

obtained in most conditions, ranging from 71 to 100% (Table 1), especially when high iron and H$_2$O$_2$ concentrations are used. The high dechlorination is also denoted by the high value of the independent parameter of Eq. (4) (97.03). When comparing the mineralization and dechlorination percentages for the different experimental conditions, it is observed that percentages of dechlorination are always higher than mineralization. This is explained by the fact that dechlorination is the first step in the mineralization process as a result of electrophilic addition of $^{\bullet}$OH leading to generation of hydroquinone [19]. Therefore, the dechlorination step is not very limited by reaction conditions such as path length or even iron and H$_2$O$_2$ concentrations as is the mineralization. The high chloride release is an important result considering the high toxicity of chlorinated compounds [2]. When aiming for the abatement of toxicity prior to further biological treatment it is possible to use low concentrations of Fe(NO$_3$)$_3$ and H$_2$O$_2$, reducing the cost of the process, as well as increased solution path length, reducing the area necessary for application of wastewater treatment. When comparing the contour plots obtained for mineralization (Fig. 1A–C) with those obtained for chloride release (Fig. 1D–F) similar behaviors are observed, e.g. the tendency for higher percentages, except for
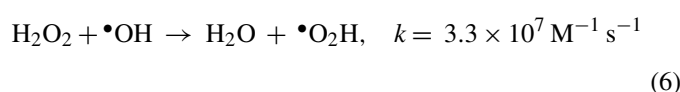
the path length and H$_2$O$_2$ correlation (Fig. 1F) which denotes no limitation of path length since high H$_2$O$_2$ concentration is provided.

It is important to mention that no mineralization or dechlorination of 4-CP was observed when the solutions were exposed to 40 min solar irradiation in the absence of iron and H$_2$O$_2$, indicating that no losses due to evaporation or photolysis of 4-CP occurred. However, 3.7% dechlorination of 4-CP was obtained under solar irradiation in the presence of only H$_2$O$_2$ and 11.5% in the presence of only Fe(NO$_3$)$_3$, for an UV dose of 2.02 J cm^{-2} (between 13 and 15 min). The low solar irradiance below 400 nm results in very low photolysis of H$_2$O$_2$, which explains the low degradation in the absence of Fe(NO$_3$)$_3$. On the other hand, the generation of $^{\bullet}$OH through photolysis of the iron complex (reaction 2) contributes to the degradation of 4-CP, resulting in 11.5% dechlorination. In the dark, total dechlorination of 4-CP (1.0 mM; TOC = 72 mg L^{-1}) and 27.8% mineralization was observed in the presence of both H$_2$O$_2$ (10 mM) and Fe(NO$_3$)$_3$ (1.0 mM) after 10 min. The high dechlorination of 4-CP in the dark may be related to the production of quinone, which acts as electron transfer reducing Fe^{3+} to Fe^{2+}, consequently improving the degradation [20].

Table 2
Ranges determined for a maximum efficiency of photo-Fenton reaction for 4-CP and comparison between the experimental results obtained under optimized conditions and theoretical results determined by the models

Compound	Response	Optimum ranges determined			Experimental conditions			Results	
		[Fe^{3+}] mM	[H$_2$O$_2$] mM	Solution path length (cm)	[Fe^{3+}] mM	[H$_2$O$_2$] mM	Solution path length (cm)	Experimental	Theoretical
4-CP	Mineralization (TOC)	1.42–1.50	18.3–20.0	4.5–4.8	1.5	20.0	4.5	81.1	79.6
4-CP	Dechlorination	0.97–1.50	14.3–20.0	4.5–9.2	1.5	20.0	4.5	100	96.7

When comparing the optimum ranges of mineralization and chloride release for the variables studied (Table 2), it is observed that, in both cases, high concentrations of Fe^{3+} and H_2O_2 favor the degradation. Previous work has shown the detrimental effect of concentrations of iron and H_2O_2 above 1.0 and 25 mM, respectively, on the degradation of herbicides, mainly due to decomposition of H_2O_2 to oxygen and water (Eq. (5)) and the scavenging of $^{\bullet}OH$ by excess H_2O_2 (Eq. (6)). The drawback of high iron concentration is that the tendency for iron precipitation increases with concentration and can hinder the transmittance of light necessary for the photo-Fenton process due to the solution turbidity, as previously reported [21]. However, under the conditions used in this work, no precipitation of iron or detrimental effect of H_2O_2 concentration was observed in the degradation of 4-CP.

$$2H_2O_2 \rightarrow 2H_2O + O_2 \qquad (5)$$

$$H_2O_2 + {}^{\bullet}OH \rightarrow H_2O + {}^{\bullet}O_2H, \quad k = 3.3 \times 10^7 \, M^{-1} \, s^{-1} \qquad (6)$$

Experiments were performed to test the optimized ranges of the three variables studied obtained by the mathematical model. The comparison between the theoretical and experimental results of 4-CP photodegradation obtained under optimized conditions show a very good agreement, considering the standard deviations of $\pm 1.9\%$ for TOC and 3.1% for dechlorination. As shown in Table 2, the theoretical and experimental values for TOC removal were 79.6% and 81.1%, respectively, while for dechlorination were 96.7% and 100% for $2.02 \, J \, cm^{-2}$ UV dose. Under optimized conditions, an UV dose of $3.15 \, J \, cm^{-2}$ (17 min solar irradiation) was sufficient to reduce by 91% a $72 \, mg \, C \, L^{-1}$ solution of 4-CP, while total dechlorination was achieved under $1.14 \, J \, cm^{-2}$ (between 5 and 7 min solar irradiation) (Fig. 2). Further degradation could probably be achieved with fresh addition of H_2O_2, which was completely consumed with an UV dose

of $3.50 \, J \, cm^{-2}$, already observed in previous work [17]. The pseudo-first order constant of H_2O_2 decomposition was calculated according to the literature [22] ($\ln[H_2O_2]/[H_2O_2]_0$ versus irradiation time) for the optimized conditions with a value of $4.24 \, s^{-1}$ for a 20 mM initial concentration of H_2O_2, what denotes the fast consumption of this reagent.

With the results obtained in this work, it is possible to estimate that in a 0.045 m deep reactor with a small area of $10 \, m^2$, $15 \, m^3/day$ (summer) and $7 \, m^3/day$ (winter) of wastewater can be treated during 10 and 8 h irradiation, respectively, reaching 90% mineralization.

4. Conclusions

The efficiency of 4-CP photodegradation was examined using multivariate analysis, with experimental results obtained under optimized conditions being very close to the expected theoretical results evidencing the reliability of the design. The solution path length plays a negative role in the mineralization percentage of 4-CP. The iron concentration plays a very important role in the degradation process of 4-CP, which can be adjusted to compensate the negative effect of solution path length. Under optimized conditions around 91% of the total initial organic carbon was removed and a total chloride release was achieved after 17 min irradiation ($3.15 \, J \, cm^{-2}$). The results of this research indicate that photo-Fenton/solar treatments achieve important levels of mineralization, with low energy costs due to solar energy application.
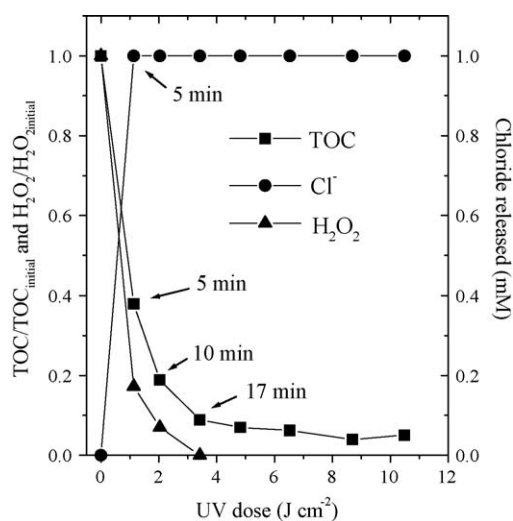
Fig. 2. Relative TOC and hydrogen peroxide concentration during solar irradiation of 4-CP under optimized conditions. Initial concentrations: 4-CP = 1.0 mM (TOC = $72 \, mg \, L^{-1}$); $Fe(NO_3)_3$ = 1.5 mM; H_2O_2 = 20.0 mM; and 4.5 cm of path length.

References

[1] Ph. Howard, Handbook of Environmental Degradation Rates, Lewis Publishers, MI, 1991.

[2] R. Crompton, Toxicants in the Aqueous Ecosystem, Wiley, UK, 1997.

[3] L.H. Keith, W.A. Telliard, Priority pollutants. I. A perspective view, Environ. Sci. Technol. 13 (1979) 416–423.

[4] R.T. Meijers, E.J. Oderwaldmuller, P. Nuhn, J.C. Kruithof, Degradation of pesticides by ozonation and advanced oxidation, Ozone Sci. Eng. 17 (1995) 673–686.

[5] P. Roche, M. Prados, Removal of pesticides by use of ozone or hydrogen peroxide ozone, Ozone Sci. Eng. 17 (1995) 657–672.

[6] S. Lehr, W.E. Glassgen, H. Sandermann, F. Beese, I. Scheunert, Metabolism of isoproturon in soils originating from different agricultural management systems and in cultures of isolated soil bacteria, Int. J. Environ. Anal. Chem. 65 (1996) 231–243.

[7] E. Wittmann, P. Cote, C. Medici, J. Leech, A.G. Turner, Treatment of a hard borehole water containing low levels of pesticide by nanofiltration, Desalination 119 (1998) 347–352.

[8] F.J. Benitez, J. Beltrán-Heredia, J.L. Acero, F.J. Rubio, Contribution of free radicals to chlorophenols decomposition by several advanced oxidation techniques, Chemosphere 41 (2000) 1271–1277.

[9] M. Pera-Titus, V. Garcia-Molina, M.A. Banos, J. Gimenez, S. Esplugas, Degradation of chlorophenols by means of advanced oxida-

tion processes: a general review, Appl. Catal. B 47 (2004) 219–256.

[10] H. Fallmann, T. Krutzler, R. Bauer, S. Malato, J. Blanco, Applicability of the photo-Fenton method for treating water containing pesticides, Catal. Today 54 (1999) 309–319.

[11] R.F.P. Nogueira, A.G. Trovó, D.F. Modé, Solar photodegradation of dichloroacetic acid and 2,4-dichlorophenol using an enhanced photo-Fenton process, Chemosphere 48 (2002) 385–391.

[12] R.F.P. Nogueira, M.R.A. Silva, A.G. Trovó, Influence of the iron source on the solar photo-Fenton degradation of different classes of organic compounds, Sol. Energy 79 (2005) 384–392.

[13] S. Göb, E. Oliveros, S.H. Bossmann, A.M. Braun, C.A.O. Nascimento, R. Guardani, Optimal experimental design and artificial neural networks applied to the photochemically enhanced Fenton reaction, Water Sci. Technol. 44 (2001) 339–345.

[14] M. Perez, F. Torrades, J. Peral, C. Lizama, C. Bravo, S. Casas, J. Freer, H.D. Mansilla, Multivariate approach to photocatalytic degradation of a cellulose bleaching effluent, Appl. Catal. B 33 (2001) 89–96.

[15] R.F.P. Nogueira, A.G. Trovó, W.C. Paterlini, Evaluation of the combined solar TiO2/photo-Fenton process using multivariate analysis, Water Sci. Technol. 49 (2004) 195–200.

[16] W.C. Paterlini, R.F.P. Nogueira, Multivariate analysis of photo-Fenton degradation of the herbicides tebuthiuron, diuron and 2,4-D, Chemosphere 58 (2005) 1107–1116.

[17] R.F.P. Nogueira, J.R. Guimarães, Photodegradation of dichloroacetic acid and 2,4-dichlorophenol by ferrioxalate/H$_2$O$_2$ system, Water Res. 34 (2000) 895–901.

[18] R.F.P. Nogueira, M.C. Oliveira, W.C. Paterlini, Simple and fast spectrophotometric determination of H$_2$O$_2$ in photo-Fenton reactions using metavanadate, Talanta 66 (2005) 86–91.

[19] O. Legrini, E. Oliveros, A.M. Braun, Photochemical processes for water treatment, Chem. Rev. 93 (1993) 671–698.

[20] R. Chen, J.J. Pignatello, Role of quinone intermediates as electron shuttles in Fenton and photoassisted Fenton oxidations of aromatic compounds, Environ. Sci. Technol. 31 (1997) 2399–2406.

[21] S. Parra, V. Sarria, S. Malato, P. Péringer, C. Pulgarin, Photochemical versus coupled photochemical-biological flow system for the treatment of two biorecalcitrant herbicides: metobromuron and isoproturon, Appl. Catal. B 27 (2000) 153–168.

[22] R. Baciocchi, M.R. Boni, L. D'Aprile, Hydrogen peroxide lifetime as an indicator of the efficiency of 3-chlorophenol Fenton's and Fenton-like oxidation in soils, J. Hazard. Mater. 96 (2003) 305–329.